

# Improvements in NIST-F1 and a Resulting Accuracy of $\delta f/f = 0.61 \times 10^{-15}$ †

T. P. Heavner, S. R. Jefferts, E. A. Donley, J. H. Shirley, and T. E. Parker  
 Time and Frequency Division  
 National Institute of Standards and Technology  
 Boulder, CO USA

**Abstract**—Over the last several years we have made many improvements to NIST-F1 (a laser-cooled cesium fountain primary frequency standard) resulting in a reduction in the uncertainty by nearly a factor of 2 in the realization of the SI second at NIST. We recently submitted an evaluation with a combined standard fractional uncertainty of  $0.61 \times 10^{-15}$  to the BIPM (Bureau International des Poids et Mesures). The total fractional uncertainty of the evaluation (including dead time and time transfer contributions) was  $0.88 \times 10^{-15}$ . This is the smallest uncertainty in a frequency standard yet submitted to the BIPM.

**Keywords**—atomic clocks; cesium; frequency control; time measurement.

## I. INTRODUCTION

In the past several years, since the publication of a complete description of the evaluation procedure in NIST-F1 we have made many improvements [1]. While these changes individually seem minor, the net result has been significant. We routinely evaluate the accuracy of NIST-F1 with a combined standard fractional uncertainty well below  $1 \times 10^{-15}$  and recently we reported a frequency evaluation with a combined standard fractional uncertainty of  $0.61 \times 10^{-15}$ , smaller by nearly a factor of 2 than reported in [1].

This paper outlines the improvements to the physics package, laser and optics system, and control system of NIST-F1, resulting in a more reliable and robust apparatus. Presently, we achieve nearly continuous, long run times (~40 d). We discuss how the changes have affected the uncertainty budget reducing both the type A and B uncertainties. The uncertainties in the spin-exchange shift and the second-order Zeeman shift corrections have been reduced to the point that the uncertainty in the black-body shift correction is now the dominant systematic uncertainty.

Since 1999 NIST-F1 has undergone 13 formal frequency evaluations that have been submitted to the BIPM to be included in TAI (Temps Atomique International/ International Atomic Time). Comparisons made with other laser-cooled Cs fountain standards, most notably direct two-way satellite comparisons with CSF1 at PTB (Physikalisch-Technische Bundesanstalt) [2], show good agreement.

An accuracy evaluation of NIST-F1 relies on a NIST time scale AT1E [3], which the fountain uses as a flywheel oscillator during evaluations, as well as the time-transfer

†Work of the US government. Not subject to US copyright.

system that is used to submit the measurements to the BIPM. AT1E is a post-processed NIST timescale generated by use of five cavity-tuned hydrogen masers and four high-performance commercial cesium beam standards. Figure 1 is a long-term Allan deviation plot comparing NIST-F1 against AT1E, and demonstrates that the system shows white FM noise properties out to 24 d, where the stability is estimated as  $\sigma_y \sim 4 \times 10^{-16}$ . This verification of the performance of the AT1E time scale shows that the type A (statistical) uncertainties presented here are valid and justifies our methods used to measure the spin-exchange shift. The high reliability exhibited by NIST-F1, resulting in long, nearly uninterrupted runs, allows the analysis of the long-term behavior shown in Fig. 1.

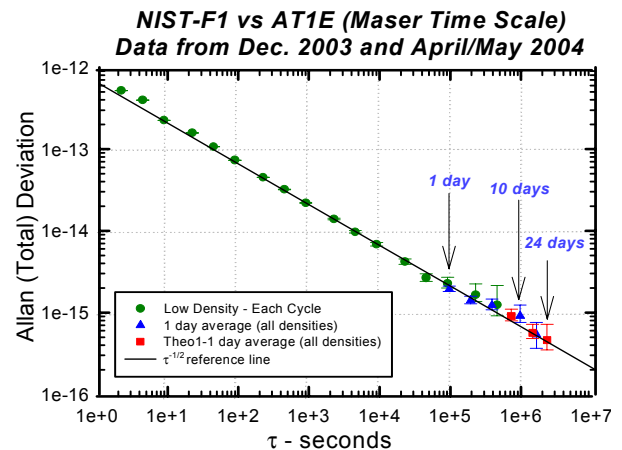


Figure 1. An Allan deviation plot comparing NIST-F1 against AT1E that demonstrates white FM noise properties out to 24 days, where the stability is estimated as  $\sigma_y \sim 4 \times 10^{-16}$ . The data at short sampling times were obtained by calculating the Allan deviation of frequency measurements from 14 days of continuous fountain operation at low atomic density. The Allan deviation at longer sampling times was calculated using the 24-hour average frequency of all individual runs. Measurements taken at high atomic densities, where the stability is better, have been included by removing the frequency offset due to the spin-exchange shift. Several points at long sampling times were calculated by use of Theo-1, a statistic designed to increase the confidence at the largest  $\tau$  values.

## II. IMPROVEMENTS MADE TO NIST-F1

### A. Laser and Optics

Since the publication of [1], the NIST-F1 laser system and the optical layout have changed considerably. The main laser system used for the optical molasses presently consists of a diode-pumped, frequency-doubled Nd:YVO<sub>4</sub> laser and provides up to 10 W of 532 nm light. This 532 nm light pumps a Ti:Sapphire ring laser that can generate more than 1 W of narrow-band light at 852 nm. The original repump laser was replaced due to a diode failure. The new repump system uses an 852 nm DBR diode to injection-lock a higher power 852 nm diode to provide ~25 mW of light that enters the fountain through a polarization-maintaining (PM) fiber-optic cable.

Both new laser systems have displayed a high level of ease of use and reliability. Lock times for the lasers are now measured in weeks. This reliability has improved statistics because our “live time”, the fraction of time in which useful data is collected divided by the intended run time, is presently ~95%. In the past, the live time was typically ~70% - 80%. This is now limited by planned shutdowns to tune up systems, software maintenance, or other rare failure modes that we have not yet addressed.

The mechanical shutters used to block resonant light during Ramsey interrogation have been greatly improved from the previous shutter design. The new system looks for proper shutter operation during each cycle of launch and measurement by measuring the light level on a photodiode monitor when the shutters are commanded to be closed. The new shutters and an improved optical layout have allowed us to reduce the uncertainty in the fluorescence light shift from  $0.2 \times 10^{-15}$  to much less than  $0.1 \times 10^{-15}$ .

### B. Optical Molasses

The new laser system provides more than twice the useful laser light power than that for the previous system. This has allowed for larger horizontal beams in the (0, 0, 1) molasses geometry while still providing enough intensity for a good optical molasses. The result is a larger optical molasses in the vertical dimension and has allowed for fountain operation with a reduced spin-exchange shift (lower density), without loss of stability.

### C. Detection Region

The laser light level in the detection zone is now servo-controlled, and this has reduced the high-frequency laser-intensity noise as well as the long-term drift in the intensity. Reduction in the long-term drift in the detection light intensity has improved the calibration of atom number and thus improved the evaluation of the Cs spin-exchange shift.

### D. Microwave Synthesis Chain and Time-Transfer into the Laboratory

The synthesizer module used to generate 9.192 GHz is the same as described in [1], but the overall synthesis chain, from maser reference to the atoms, has been modified. The addition

of a high-quality quartz B.V.A. (electrodeless) crystal oscillator in a phase-locked loop ( $\tau \approx 10$  s) has reduced the fast noise from the 100 MHz reference originating from a maser in the NIST clock ensemble. This circuit topology exhibits the superior short-term performance of the BVA crystal oscillator while maintaining the long-term stability of the maser. The improved microwave system contains a second, parallel synthesis chain that serves as an error monitor. Problems in the synthesis chain resulting in excessive phase noise are logged by software.

### E. Vacuum System

A sensitive ion gauge with a nominal base pressure of  $5 \times 10^{-12}$  torr was added to the physics package below the molasses region. This is used in conjunction with the ion pump current readings to measure the pressure within the physics package and provides added confidence on determining any possible bias due to background gases.

### F. Temperature Control

Improved temperature sensing instrumentation was added along the microwave cavity and copper flight tube, including a Pt RTD temperature sensor with an accuracy of  $\pm 0.1$  K.

### G. Control System

We have developed and are using new software to control NIST-F1 that is flexible and easy to modify while still being robust. The new software architecture has error monitoring in the form of logged digital inputs that represent the health and status of many of the fountain's subsystems. This error monitoring and detection system has allowed us to quickly fix problems and get the fountain operational again, thus increasing the “live time”.

## III. NIST TIME SCALE

The NIST clock ensemble consists of five cavity-tuned hydrogen masers and four high-performance, commercial cesium standards, and is used to generate AT1E, a post-processed time scale that has a stability of  $\sigma_y \sim 2 \times 10^{-16}$  at averaging times of 30 days, and a long-term frequency drift rate of less than  $\pm 3 \times 10^{-15}$  per year [3]. Because AT1E is exceptionally stable, and the noise properties have been well characterized, we are able to operate NIST-F1 using methods inaccessible to other fountain groups. For example, dead time in the operation of NIST-F1 results in only a small additional uncertainty to the frequency measurements and can therefore be tolerated [4].

## IV. CORRECTED SYSTEMATIC FREQUENCY BIASES

Table 1 lists the all the frequency biases considered in the accuracy evaluations of NIST-F1. The biases for which corrections are applied are discussed here.

### A. Spin-Exchange Shift

Results from various groups as well as theoretical work [5] show that the spin-exchange frequency shift is strongly energy-dependent and thus is a function of the type of Cs

source used, (MOT, molasses) and details of the atomic velocity and spatial distributions. But given that these parameters remain constant, the shift is expected to be linear with atomic density.

Presently, we use a density-extrapolation method described in [1]. Frequency measurements are made at various atomic densities, and a weighted, least-squares linear fit of the data yields an intercept and a slope that are used to correct for the spin-exchange shift and determine final uncertainties. The atomic density is set by controlling the detected atom signal. Measurements of the atomic spatial and velocity distributions in NIST-F1 show that they are constant at  $\sim 1\%$  over the range of parameters used to change the atom number, and confirm that the detected signal level is proportional to the atomic density. Coarse control of atom number is achieved by simultaneously making small changes to the molasses time, laser power, and temperature of the cesium oven. Fine control ( $\sim 1\%$ ) is achieved using a servo that locks the detected atom signal to a set point by varying the microwave power entering the state selection cavity. We operate NIST-F1 most of the time ( $\sim 70\%$ ) at a low density where the fractional spin-exchange shift is  $\delta f/f \sim 0.53(15) \times 10^{-15}$ .

TABLE I. A SUMMARY OF THE SYSTEMATIC FREQUENCY BIASES THAT ARE CONSIDERED IN NIST-F1 IN UNITS OF FRACTIONAL FREQUENCY  $\times 10^{-15}$ . THE LARGEST CONTRIBUTION TO THE FINAL UNCERTAINTY IS DUE TO THE BLACK-BODY SHIFT. THE \* IS A REMINDER THAT THE SPIN-EXCHANGE BIAS IS NOT CONSTANT DURING AN EVALUATION, AND THE VALUE SHOWN BELOW IS THE BIAS AT LOW ATOMIC DENSITY, AT WHICH NIST-F1 OPERATES  $\sim 70\%$  OF THE TIME.

Physical Effect	Bias	Type B Uncertainty
Second-Order Zeeman	+36.46	0.10
Second-Order Doppler	<0.1	<0.1
Cavity Pulling	<0.1	<0.1
Rabi Pulling	<0.01	<0.1
AC Zeeman (heaters)	<0.1	<0.1
Cavity Phase (distributed)	<0.1	<0.1
Fluorescence Light Shift	<0.1	<0.1
Adjacent Transitions	<0.1	<0.1
Spin Exchange	(-0.53)*	(0.15)*
Black-body	-21.21	0.26
Gravitation	+180.54	0.10
RF Spectral Purity	0	<0.1
Integrator Offset	0	<0.1
AM on Microwaves	0	<0.1
Microwaves	0	0.14
Total Type B Standard Uncertainty		0.33

### B. Second-Order Zeeman

In [1] we described the methods that we use for determining the second-order Zeeman shift correction in NIST-F1. Two complementary methods using magnetic field-sensitive transitions in Cs were described. In [1] we stated a fractional uncertainty in the second-order Zeeman correction of  $0.3 \times 10^{-15}$ , which corresponds to an uncertainty of  $\pm 1$  fringe on the  $|3,1\rangle \rightarrow |4,1\rangle$  manifold. This was an overly conservative uncertainty since the two methods agree to within

$0.04 \pm 0.05$  fringes. Presently, we state an uncertainty on the second-order Zeeman shift of  $0.1 \times 10^{-15}$  that reflects the use of a smaller magnetic field, confidence that the fringe location is known to much better than  $\pm 1$  fringe, and long-term measurements on the  $|3,1\rangle \rightarrow |4,1\rangle$  transitions, which show a level of magnetic field noise corresponding to a fractional frequency shift of  $\delta f/f < 10^{-17}$  on the  $|3,0\rangle \rightarrow |4,0\rangle$  transition.

### C. Black-body Shift

While we have improved the temperature-sensing instrumentation and reduced temperature gradients along the copper microwave cavity and time-of-flight structure, the uncertainty in the blackbody shift in NIST-F1 still reflects an uncertainty of  $\pm 1$  K in the radiation environment as seen by the atoms. Presently, we report a fractional black-body shift correction of  $-21.21 \times 10^{-15}$  with an uncertainty in the correction of  $0.26 \times 10^{-15}$ . This is now the largest type B uncertainty for NIST-F1.

### D. Gravitational Redshift

The gravitational redshift is the largest clock shift in NIST-F1. Improved models of the geoid [6] have resulted in a more precise determination of the gravitational potential at the location of NIST-F1 in Boulder, Colorado. The uncertainty stated in this latest work is  $\pm 0.3 \times 10^{-16}$ , which corresponds to an uncertainty of 30 cm with respect to the geoid. We presently state a fractional uncertainty of  $1.0 \times 10^{-16}$  for NIST-F1.

TABLE II. THE FINAL UNCERTAINTY BUDGET FROM THE APRIL-JUNE 2004 EVALUATION OF NIST-F1 INCLUDING DEAD TIME,  $u_{\text{LINK/LAB}}$ , AND TIME-TRANSFER,  $u_{\text{LINK/TAI}}$ , CONTRIBUTIONS.

Stability $u_A$	$0.51 \times 10^{-15}$
Systematic $u_B$	$0.33 \times 10^{-15}$
Combined $u_A$ and $u_B$	$0.61 \times 10^{-15}$
Link to Clock $u_{\text{link/lab}}$	$0.40 \times 10^{-15}$
Link to TAI $u_{\text{link/TAI}}$	$0.50 \times 10^{-15}$
Final Uncertainty into TAI	$0.88 \times 10^{-15}$

## V. UNCORRECTED FREQUENCY BIASES

The uncorrected frequency biases in Table 1 have been evaluated using leveraged measurements, theoretical modeling, or a combination of both to determine that they contribute a fractional shift of less than  $10^{-16}$ . These shifts have been discussed thoroughly in [1]. In light of the overall reduction in the type A and type B uncertainties in NIST-F1, these small biases have been reconsidered [7].

## VI. NIST-F1 PERFORMANCE IN TAI

Table 2 lists the type A and type B uncertainties of the most recent accuracy evaluation of NIST-F1 and additional uncertainties due to NIST-F1 dead-time,  $u_{\text{link/lab}}$ , and the link into TAI,  $u_{\text{link/TAI}}$ . The accuracies reported by NIST-F1 are supported by comparisons with other Cs fountain frequency standards. Figure 2 shows the long-term performance of NIST-F1 and other standards with respect to TAI.

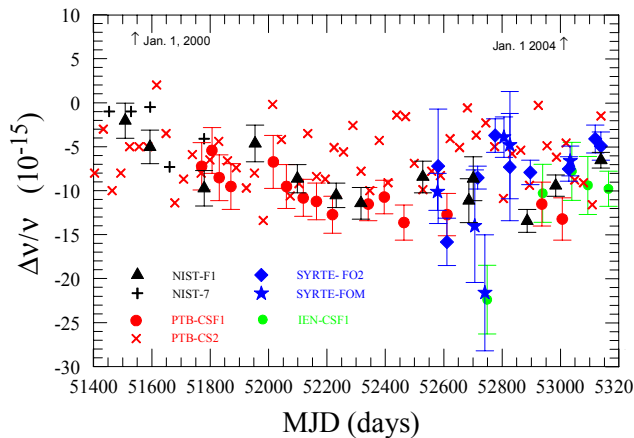


Figure 2. The long-term performance of NIST-F1 and other Cs fountain frequency standards with respect to TAI (Temps Atomique International/International Atomic Time).

## VII. CONCLUSION

The improvements outlined here have made NIST-F1 a very reliable apparatus capable of long, nearly continuous run times. Both the type A and type B uncertainties of accuracy evaluations have been reduced. Specifically, the uncertainties in both the spin-exchange and second-order Zeeman shift corrections are no longer dominant. Rather, the uncertainty in the black-body shift correction is now the largest contributor to the type B uncertainty budget. Recently, we reported an evaluation with a combined standard fractional uncertainty of  $0.61 \times 10^{-15}$ , which was submitted to the BIPM with a total fractional uncertainty (including dead time and time transfer

contributions) of  $0.88 \times 10^{-15}$ . This is the smallest uncertainty in a frequency standard yet submitted to the BIPM.

## ACKNOWLEDGMENT

The authors thank Mike Lombardi and David R. Smith for valuable comments on this manuscript.

## REFERENCES

- [1] S.R. Jefferts, J.H. Shirley, T.E. Parker, T.P. Heavner, D.M. Meekhof, C.W. Nelson, F. Levi, G. Costanzo, A. DeMarchi, R.E. Drullinger, L. Hollberg, W.D. Lee, and F.L. Walls, "Accuracy Evaluation of NIST-F1", *Metrologia*, vol. 39, pp. 321-336, 2002.
- [2] T.E. Parker, P. Hetzel, S.R. Jefferts, S. Weyers, L.M. Nelson, A. Bauch, and J. Levine, "First Comparison of Remote Cesium Fountains", *Proc. 2001 IEEE Intl. Freq. Cont. Symp.*, pp. 63-68, 2001.
- [3] T.E. Parker, "Performance of a Hydrogen Maser Ensemble and Characterization of Frequency Standards", *Proc. 1999 Joint Mtg. IEEE Intl. Freq. Cont. Symp. and EFTF Conf.*, pp. 173-176, 1999.
- [4] T.E. Parker, "Comparing and Evaluating the Performance of Primary Standards: Impact of Dead Time", *Proc. 2001 IEEE Intl. Freq. Cont. Symp.*, pp. 57-62, 2001.
- [5] P.J. Leo, P.S. Julienne, F.H. Mies, and C.J. Williams, "Collisional Frequency Shifts in  $^{133}\text{Cs}$  Fountain Clocks", *Phys. Rev. Lett.*, vol. 86, no. 17, pp. 3743-3746, 2001.
- [6] N.K. Pavlis and M.A. Weiss, "The Relativistic Redshift with  $3 \times 10^{-17}$  Uncertainty at NIST, Boulder, Colorado, USA", *Metrologia*, vol. 40, pp. 66-73, 2003.
- [7] T.P. Heavner, E.A. Donley, J. Shirley, S.R. Jefferts, T.E. Parker, *to be submitted to Metrologia*.